GCOM-C/SGLI
Lunar Calibration Evaluation

Taichiro Hashiguchi[a], Tomoyuki Urabe[b], Shigemasa Ando[b], Yoshihiko Okamura[b], Kazuhiro Tanaka[b], Arata Okuyama[c]

[a]Remote Sensing Technology Center of Japan (RESTEC)
[b]Japan Aerospace Exploration Agency (JAXA)
[c]Japan Meteorological Agency (JMA)

This work is based on a contract with JAXA (JX-PSPC-523224), and complies with GIRO usage policy, "Global Satellite Inter-Calibration System, GIRO and GSICS Lunar Observation Dataset Usage Policy", Version 1.0, May 2015, GSICS-RD005.

Contents

1. Introduction
   - GCOM-C/SGLI overview
   - SGLI specification

2. SGLI Lunar calibration
   - SGLI Lunar calibration operation
   - Analysis method of SGLI lunar calibration
   - Time-series trend results
   - Inter-comparison of the onboard calibration

3. Derivation of Calibration Coefficient
   - Correction of phase angle dependence
   - Validation using AHI

4. Conclusion

GCOM-C overview

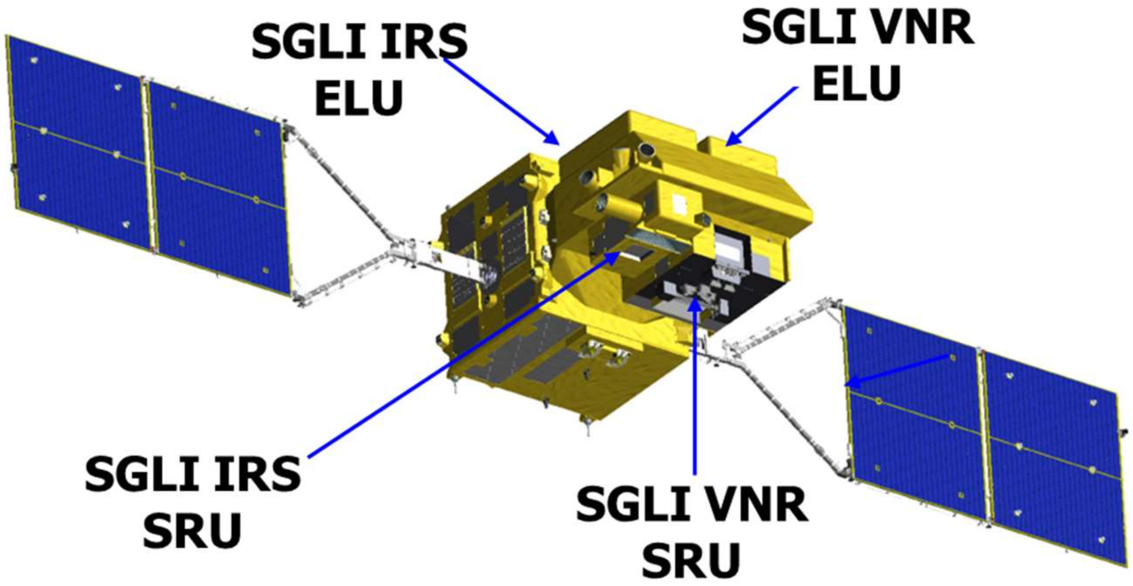

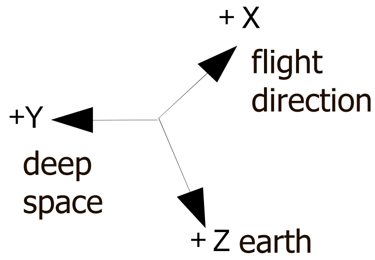

SGLI	**Second-generation Global Imager**
VNR	**Visible and Near Infrared Radiometer**
IRS	**Infrared Scanning Radiometer**
SRU	**Scanning Radiometer Unit**
ELU	**Electronic Unit**

- GCOM-C was successfully launched on December 23, 2017 and is continuing regular observation operations.
- The various GCOM-C scientific products have been released to public since December, 2018. [Data access --> https://gportal.jaxa.jp/]

Second-generation Global Imager (SGLI) Overview

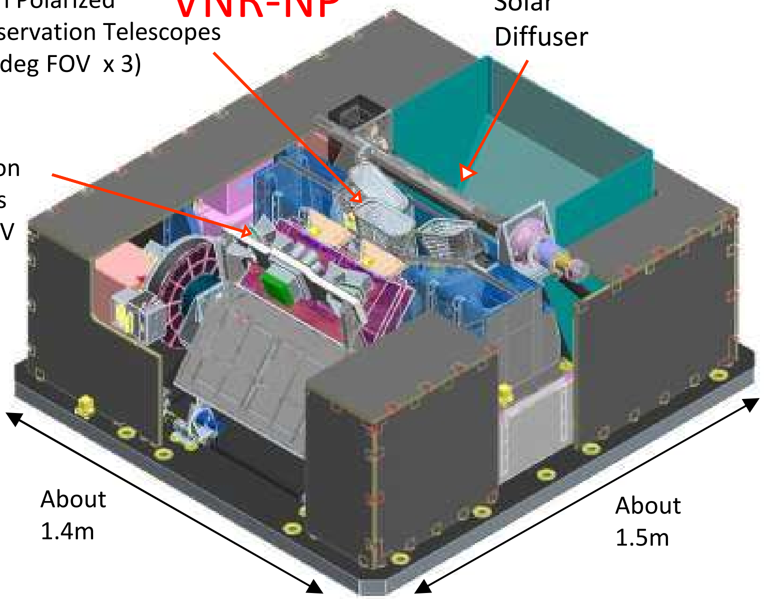

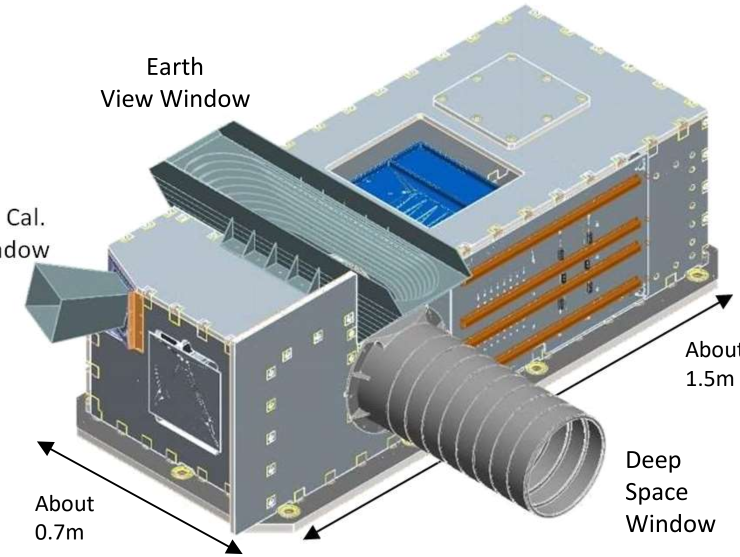

Visible and Near Infrared Radiometer
(SGLI-VNR)

Infrared Scanning Radiometer
(SGLI-IRS)

- VNR-NP consists of three 24-degree-FOV telescopes configured in cross track direction to realize the wide FOV (70 degrees).
- VNR-PL has the tilting mechanism to observe around ±45 degrees in along track direction.

- The combination of the 45 degrees tilting scanning mirror and Ritchey-Chretien type telescope realize the wide 80 degrees FOV observation swath.

SGLI Specification

- The SGLI features are **250m (VNR-NP & SW3) and 250/500m (TIR) spatial resolution** and **polarization/along-track slant view** channels (VNR-PL), which will improve land, coastal, and aerosol observations.

GCOM-C SGLI characteristics	
Orbit	Sun-synchronous (descending local time: 10:30) Altitude 798km, Inclination 98.6deg
Mission Life	5 years
Scan	Push-broom electric scan (VNR) Wisk-broom mechanical scan (IRS)
Scan width	1150km cross track (VNR-NP & VNR-PL) 1400km cross track (IRS-SWI & IRS-TIR)
Digitalization	12bit
Polarization	3 polarization angles for VNR-PL
Along track direction	Nadir for VNR-NP, IRS-SWI and IRS-TIR, +45 deg and -45 deg for VNR-PL
On-board calibration	VNR-NP, VNR-PL: Solar diffuser, LED, Lunar cal. maneuvers, and dark current by masked pixels and nighttime obs. IRS-SWI: Solar diffuser, LED, Lunar, and dark current by deep space window IRS-TIR: Black body and dark current by deep space window

250m over the Land or coastal area, and 1km over offshore

Multi-angle obs. for 673.5nm and 868.5nm

SGLI channels							
	CH	λ	$\Delta\lambda$	L_{std}	L_{max}	SNR at Lstd	IFOV
		VNR-NP, VNR-PL, IRS-SWI: nm IRS-TIR: μm		VNR-NP, VNR-PL, IRS-SWI :W/m²/sr/μm IRS-TIR: Kelvin		VNR-NP, VNR-PL, IRS-SWI : SNR IRS-TIR: NEΔT	m
VNR-NP	VN1	380	10	60	210	250	250
	VN2	412	10	75	250	400	250
	VN3	443	10	64	400	300	250
	VN4	490	10	53	120	400	250
	VN5	530	20	41	350	250	250
	VN6	565	20	33	90	400	250
	VN7	673.5	20	23	62	400	250
	VN8	673.5	20	25	210	250	250
	VN9	763	12	40	350	1200	250/1000
	VN10	868.5	20	8	30	400	250
	VN11	868.5	20	30	300	200	250
VNR-PL	P1	673.5	20	25	250	250	1000
	P2	868.5	20	30	300	250	1000
IRS-SWI	SW1	1050	20	57	248	500	1000
	SW2	1380	20	8	103	150	1000
	SW3	1630	200	3	50	57	250
	SW4	2210	50	1.9	20	211	1000
IRS-TIR	T1	10.8	0.7	300	340	0.2	250/1000
	T2	12.0	0.7	300	340	0.2	250/1000

TIR: 500m resolution is also used

Lunar Calibration Operation

- ✓ The lunar observation images are captured by maneuvering GCOM-C attitude around the pitch axis.
- ✓ Pitch maneuver rate is 0.15 degree/second with high stability to obtain precise oversampled lunar image in along-track direction.
- ✓ The phase angle(Sun - Moon - Satellite) is around +7+/-3degree.
  - Lunar calibration concept is similar to SeaWiFS.

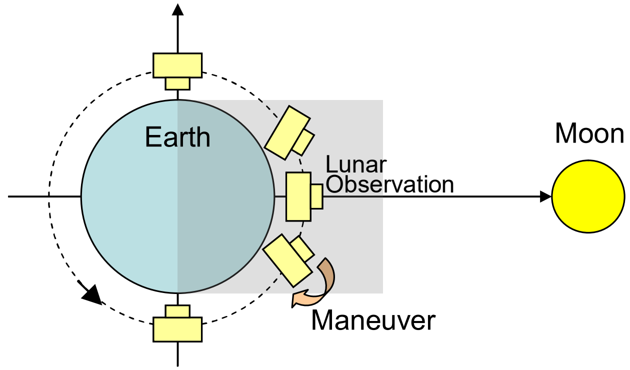

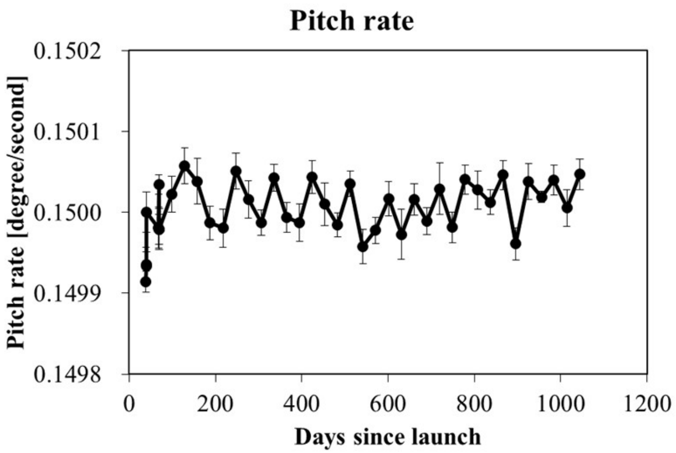

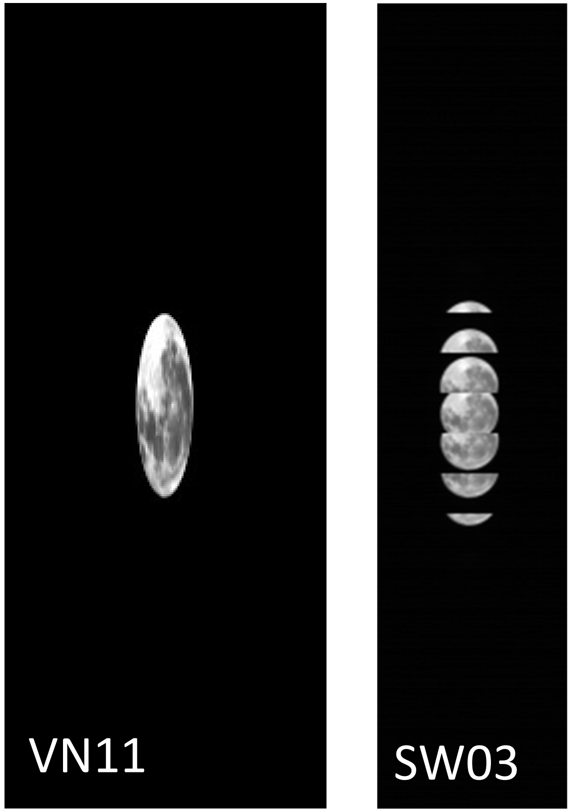

Analysis Method (VNR)

- <u>Analysis method of SGLI lunar calibration data</u>

[Case of VNR-NP/PL]

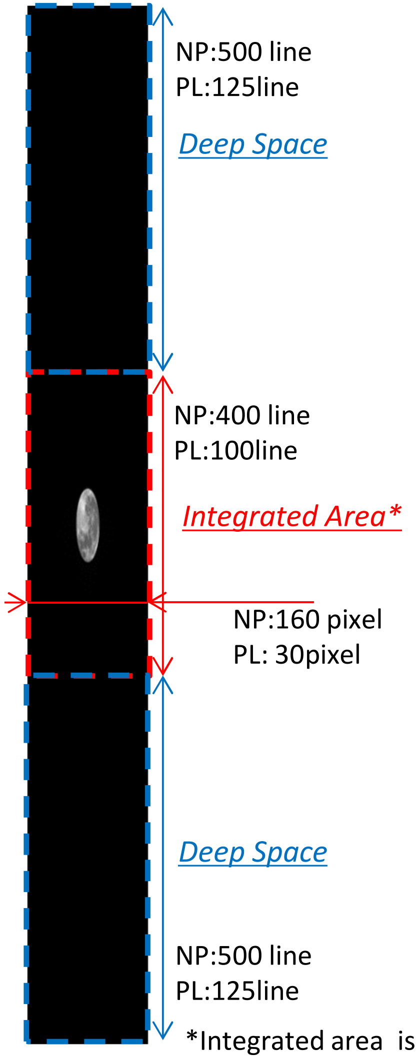

- ✓ Removes dark noise using averaging deep space data per pixel.
- ✓ Converts to radiance image $L_{k,p}$ using radiometric parameter.
- ✓ To compare with lunar irradiance model, the radiance is converted to integrated lunar irradiance I_k using following equation.

$$I_k{}^{SGLI} = \left(\sum_{p=1}^{N} \Omega'_{k,p} L_{k,p} \right)$$

I_k : Lunar irradiance (k=ch1~11)
N : Total number of pixel
$\Omega'_{k,p}$: Solid angle per pixel include oversampling and $\sin\theta$ effect
θ : Angle between satellite-moon vector and satellite pitch axis

*Integrated area is defined taking into account stray light.

Analysis Method (IRS)

➢ Analysis method of SGLI lunar calibration data

[Case of IRS-SWIR]

IRS discretely captures the moon because of whisk-broom type radiometer. Therefore, in order to obtain integrated lunar irradiance, it is necessary to round the lunar image.

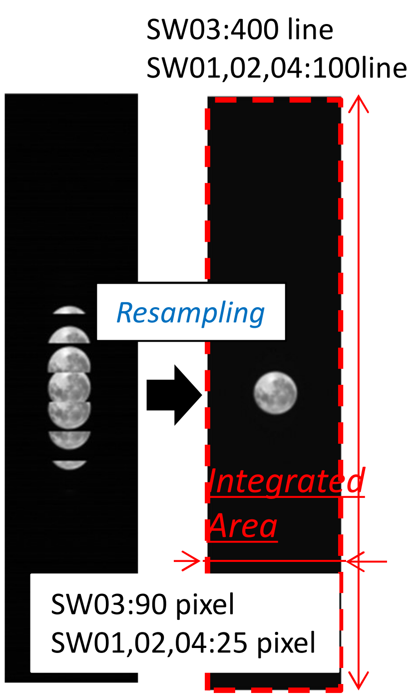

IRS-SW03

- ✓Converts to radiance image $L_{k,p}$ using radiometric parameter.
- ✓The observed pixels of each detector are projected on the AT-CT plane in consideration of line-of-sight vector and the pitch maneuver.
- ✓ Converts to irradiance image $I_{k,p}$ using the solid angle for each pixel.
- ✓ Reconstructs the lunar irradiance image from the weighted average according to the a field of view of each detector in the resampling grid.
- ✓The lunar integrated irradiance ${I_k}^{SGLI}$ is calculated.

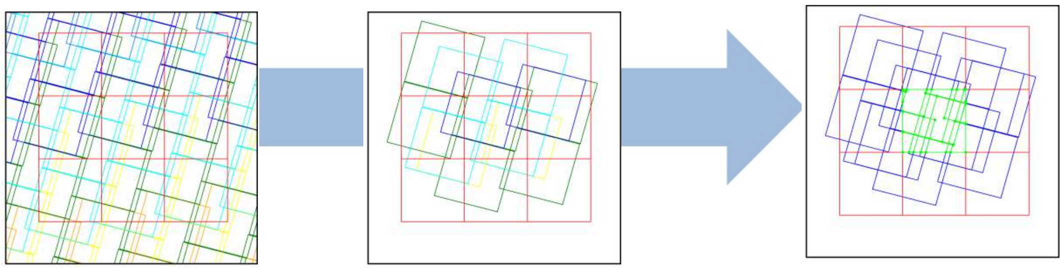

Red line: Resampling grid
※Colors show the observed pixel of each scan

Green : Weighted average pixel

Time-series trend results(VNR)

CH	VN1	VN2	VN3	VN4	VN5	VN6	VN7	VN8	VN9	VN10	VN11
WL [nm]	380	412	443	490	530	565	673.5	673.5	763	868.5	868.5

- SGLI/GIRO Time-series trend

VN01-VN06 Nadir telescope

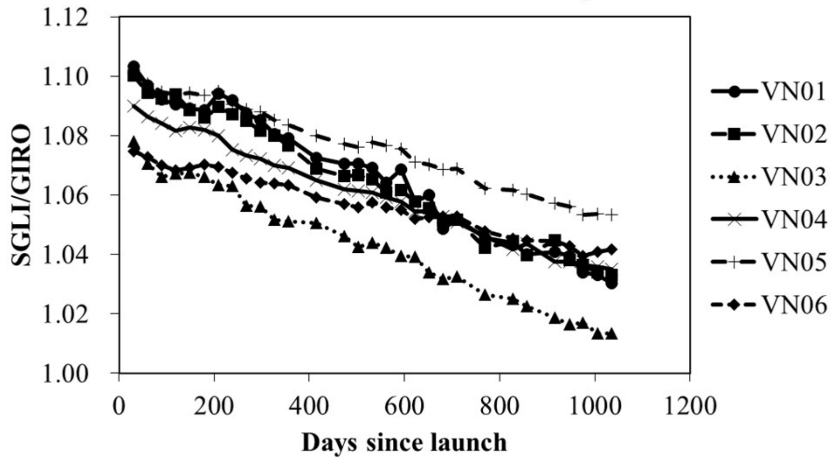

VN07-11 Nadir telescope

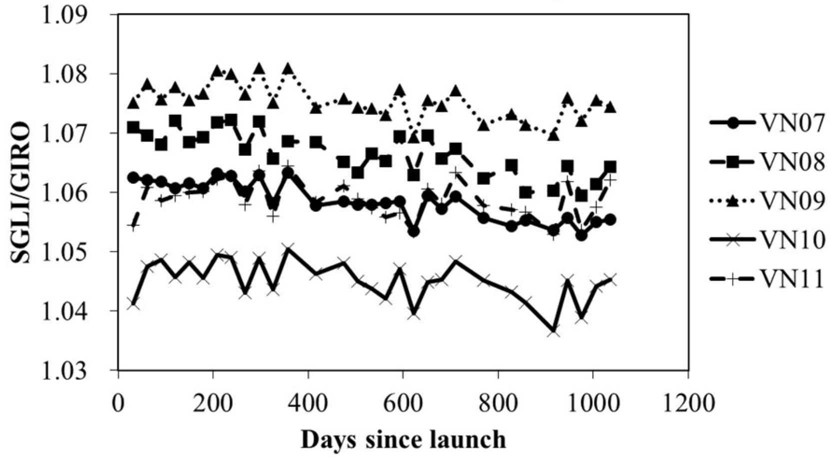

- SGLI/GIRO Time-series trend (Normalized 2018/2/1)

VN01-VN06 Nadir telescope

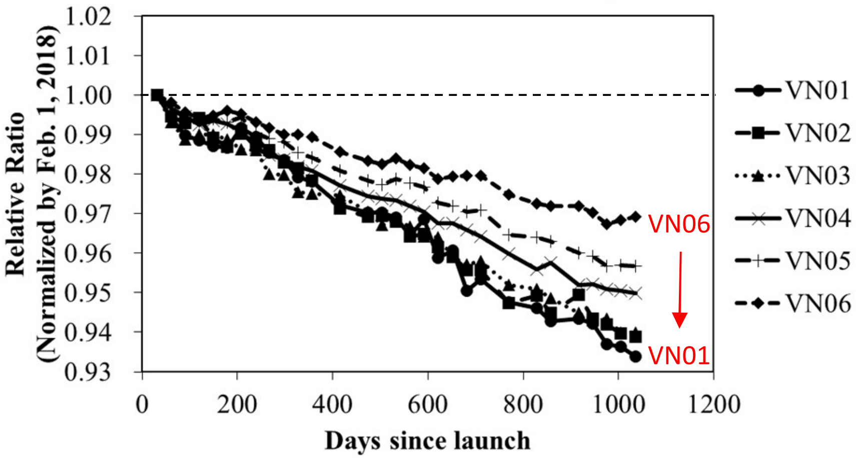

VN07-11 Nadir telescope

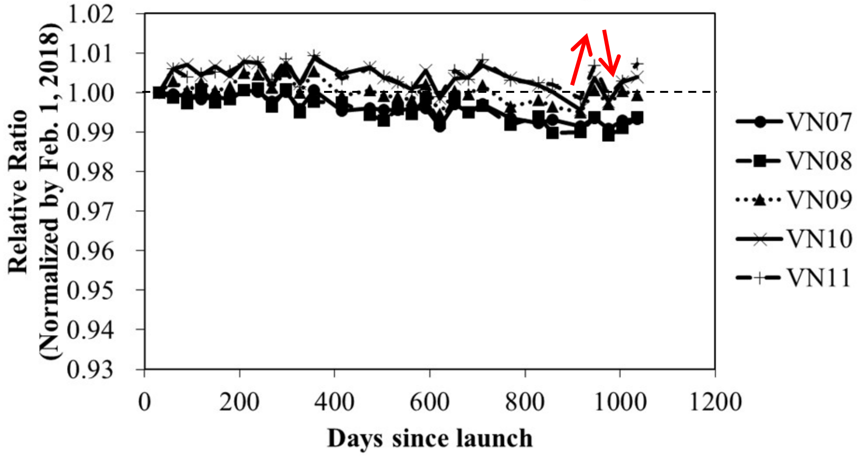

Time-series trend results(SWIR)

CH	SW1	SW2	SW3	SW4
WL [nm]	1050	1380	1630	2210

☐ SGLI/GIRO Time-series trend

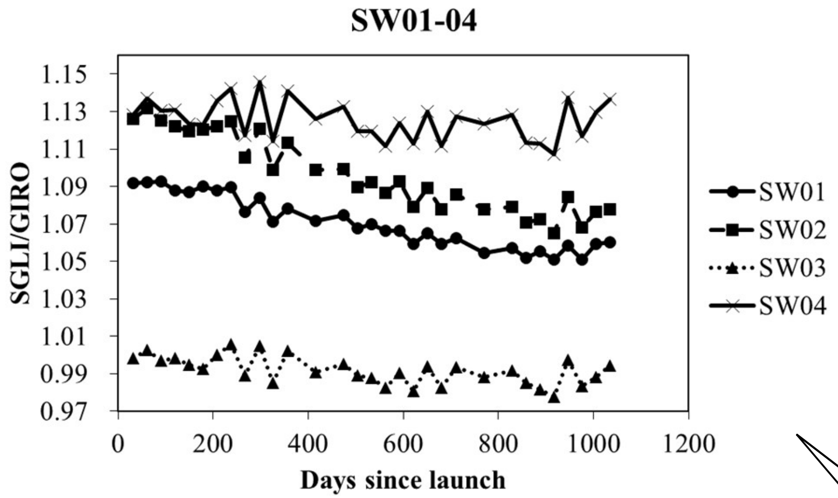

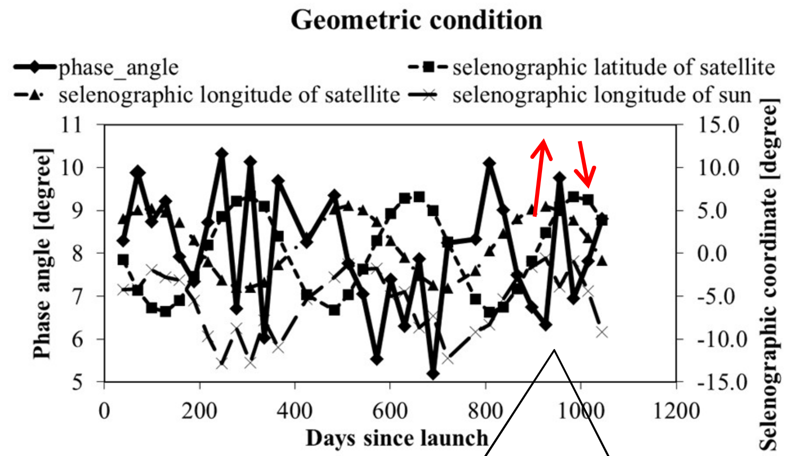

☐ SGLI/GIRO Time-series trend (Normalized 2018/2/1)

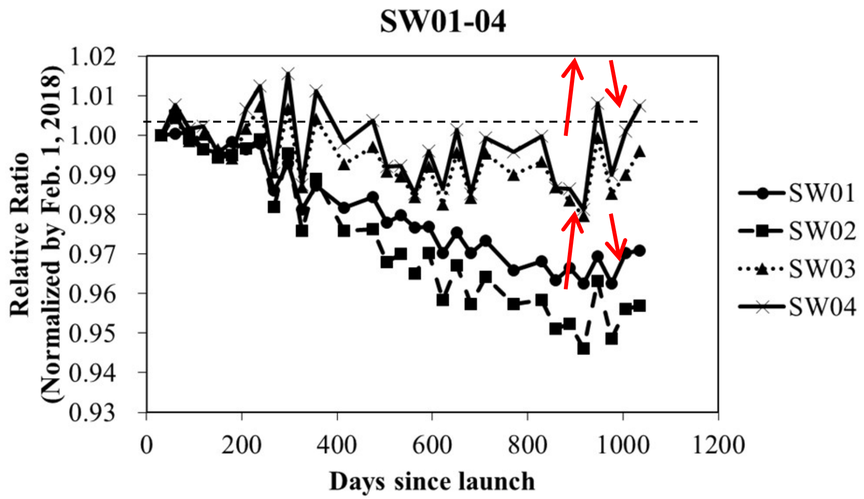

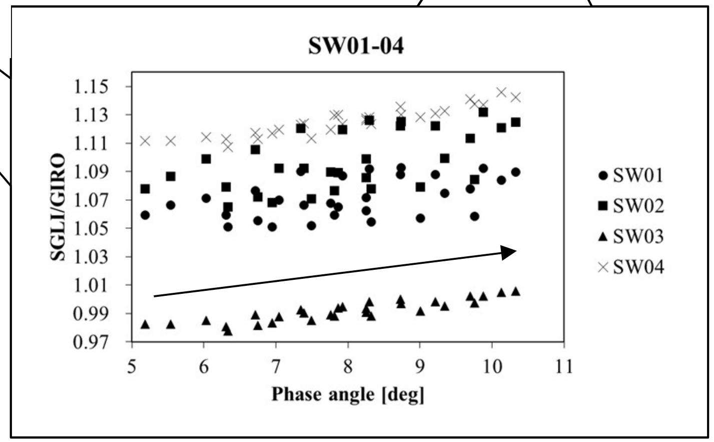

✓ These trends indicate fluctuations synchronized with the behavior of the lunar phase angle

Inter-comparison of the onboard calibration

- Inter-comparison of the onboard calibration
  - ✓ Lunar calibration
  - ✓ Solar calibration (every 8 days)
  - ✓ Internal light source calibration (every 8 days)

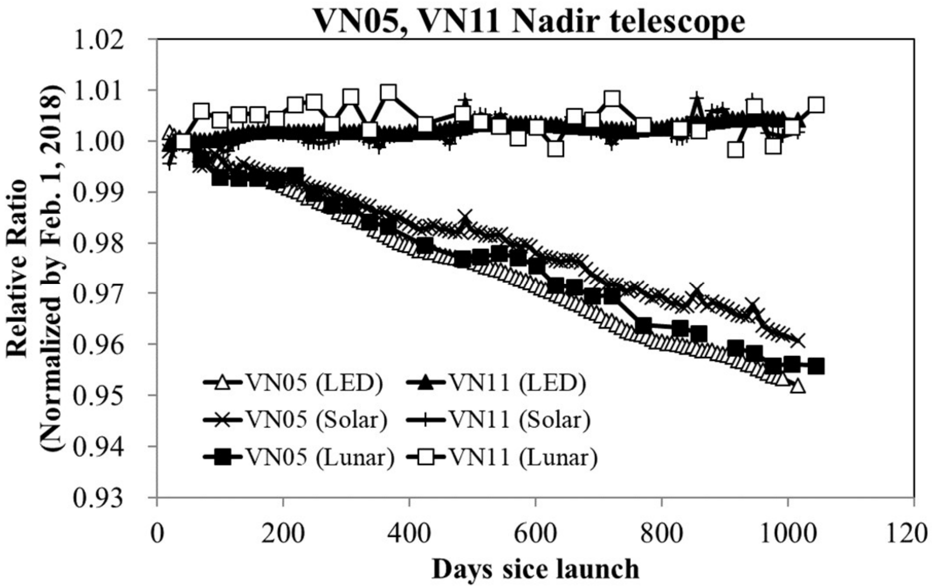

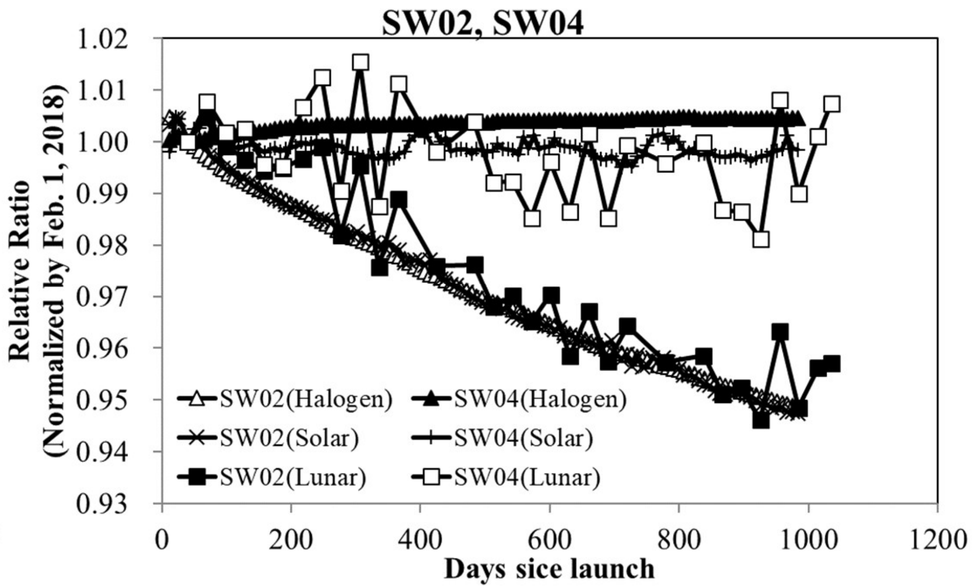

- ✓ These trends are normalized with the first lunar calibration date (February 1, 2018) for comparison.
- ✓ In VNIR and SWIR bands, the inter-comparisons between in orbit calibrations are consistent within 1.0%, and these results suggest that the lunar calibration evaluation acquires the degradation characteristics of the sensor in detail.

Derivation of Calibration Coefficient

☐ Derivation of calibration coefficient

- ✓ The SGLI/GIRO trends have a feature of phase angle dependence.
- ✓ For the construction of the simple study model, the conditions for evaluation are limited to the following:
  - ➢ The roll offset angle is 0° or 1°
  - ➢ The phase angle range is 5.0° to 11.0°
- ✓ Using the simple model shown below, the sensor responsivity degradation and phase angle dependence were separated by multiple regression analysis.

$$f_{ch,n} = a_{ch} \times g_n + b_{ch} \times d_n + c_{ch}$$

f : the SGLI/GIRO trend
g : the phase angle
d : the days since launch
n : the number of the lunar calibration
a_{ch}: the phase angle dependent coefficient
b_{ch}: the sensor degradation coefficient
c_{ch}: the constant

■ Evaluation period

- ✓ Confirmation that these characteristics do not depend on the evaluation period.

I. 2018/2-2020/1
II. 2018/10-2020/9

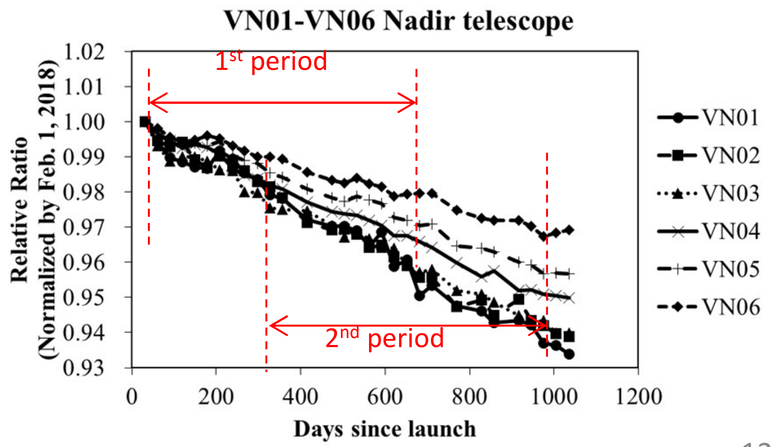

Derivation of Calibration Coefficient

- *Sensor responsivity degradation*

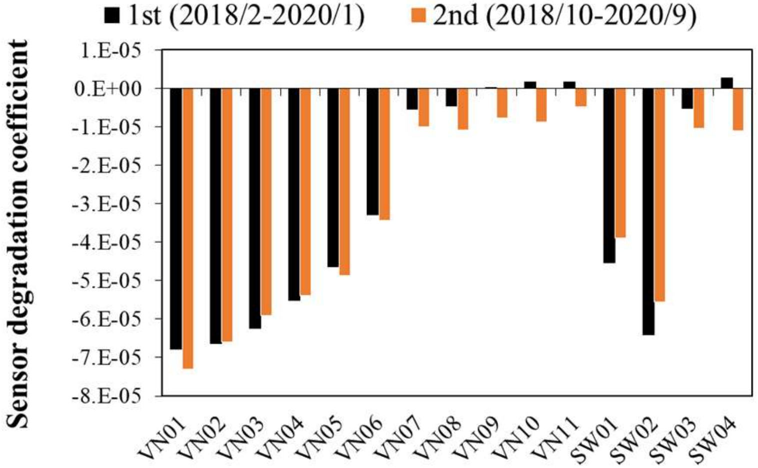

- *Phase angle dependence*

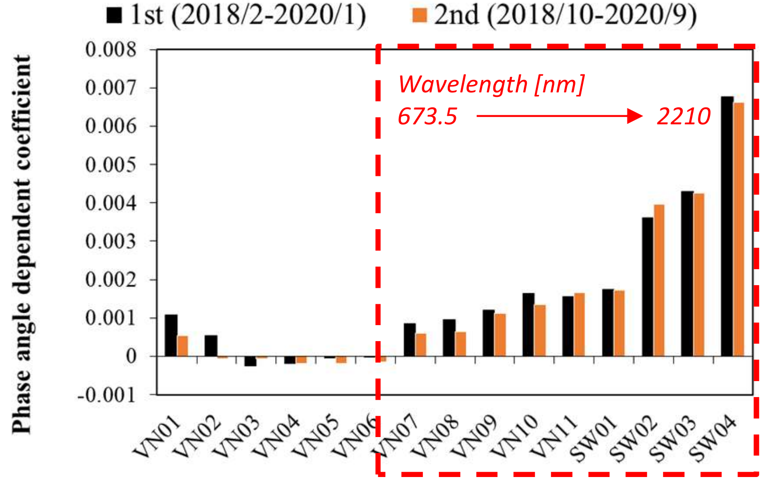

- ✓ The phase angle dependence at wavelengths longer than VN07(673.5 nm) is statistically significant.
- ✓ The dependency increases as the wavelength increases. In particular, the dependence is strong in the SWIR bands.

Band	1st evaluation period						2nd evaluation period					
	R2	RMSE	Sensor degradation dependence [1/day]		Phase angle dependence [1/degree]		R2	RMSE	Sensor degradation dependence [1/day]		Phase angle dependence [1/degree]	
			slope	p-value	slope	p-value			slope	p-value	slope	p-value
VN01	0.954	0.0031	-6.78E-05	2.54E-12	1.08E-03	7.67E-02	0.962	0.0028	-7.30E-05	4.33E-13	5.46E-04	2.93E-01
VN02	0.982	0.0018	-6.64E-05	3.19E-16	5.28E-04	1.32E-01	0.962	0.0025	-6.59E-05	3.98E-13	-7.39E-05	8.72E-01
VN03	0.975	0.0020	-6.24E-05	3.31E-15	-2.54E-04	4.89E-01	0.985	0.0014	-5.91E-05	2.23E-16	-7.49E-05	7.69E-01
VN04	0.989	0.0011	-5.51E-05	2.23E-18	-1.82E-04	3.96E-01	0.991	0.0010	-5.38E-05	2.86E-18	-1.83E-04	3.06E-01
VN05	0.973	0.0016	-4.63E-05	7.48E-15	-4.65E-05	8.70E-01	0.982	0.0013	-4.86E-05	9.43E-16	-1.81E-04	4.35E-01
VN06	0.970	0.0012	-3.29E-05	2.29E-14	-1.83E-05	9.32E-01	0.971	0.0011	-3.42E-05	4.31E-14	-1.54E-04	4.60E-01
VN07	0.591	0.0016	-5.32E-06	2.05E-02	8.58E-04	8.84E-03	0.656	0.0015	-9.96E-06	7.96E-05	6.06E-04	4.24E-02
VN08	0.625	0.0015	-4.61E-06	3.04E-02	9.55E-04	2.64E-03	0.509	0.0022	-1.07E-05	1.13E-03	6.48E-04	1.18E-01
VN09	0.459	0.0017	1.67E-07	9.42E-01	1.20E-03	1.39E-03	0.548	0.0020	-7.76E-06	5.54E-03	1.12E-03	5.58E-03
VN10	0.538	0.0021	1.60E-06	5.34E-01	1.63E-03	2.18E-04	0.615	0.0020	-8.84E-06	2.65E-03	1.34E-03	1.85E-03
VN11	0.550	0.0020	1.70E-06	4.81E-01	1.56E-03	1.65E-04	0.601	0.0020	-4.85E-06	6.32E-02	1.65E-03	2.48E-04
SW01	0.944	0.0025	-4.54E-05	7.26E-11	1.75E-03	1.55E-03	0.925	0.0024	-3.89E-05	1.05E-10	1.73E-03	6.68E-04
SW02	0.961	0.0031	-6.40E-05	1.12E-11	3.62E-03	8.90E-06	0.935	0.0034	-5.55E-05	1.13E-10	3.97E-03	4.08E-06
SW03	0.917	0.0019	-5.24E-06	6.18E-02	4.30E-03	7.53E-10	0.883	0.0023	-1.05E-05	1.24E-03	4.25E-03	6.89E-09
SW04	0.913	0.0027	2.80E-06	4.67E-01	6.76E-03	1.68E-10	0.884	0.0034	-1.10E-05	1.35E-02	6.61E-03	3.01E-09

Derivation of Calibration Coefficient

- SGLI/GIRO residual from multiple regression equation

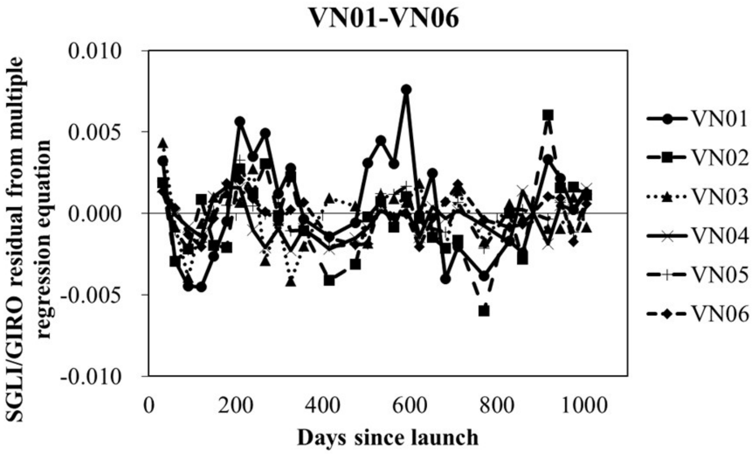

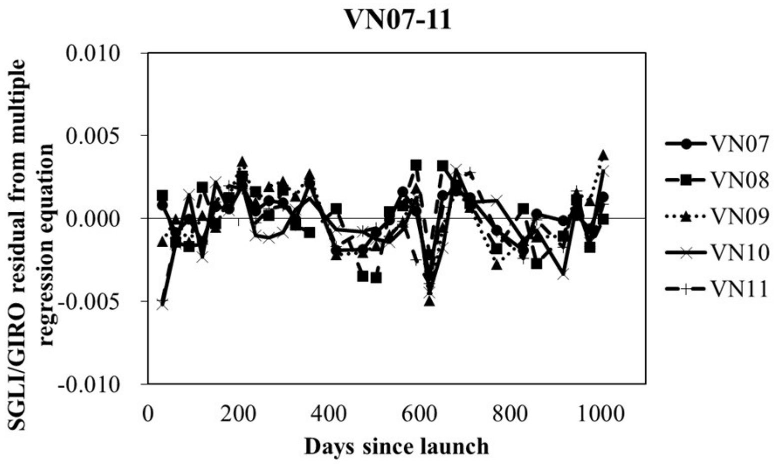

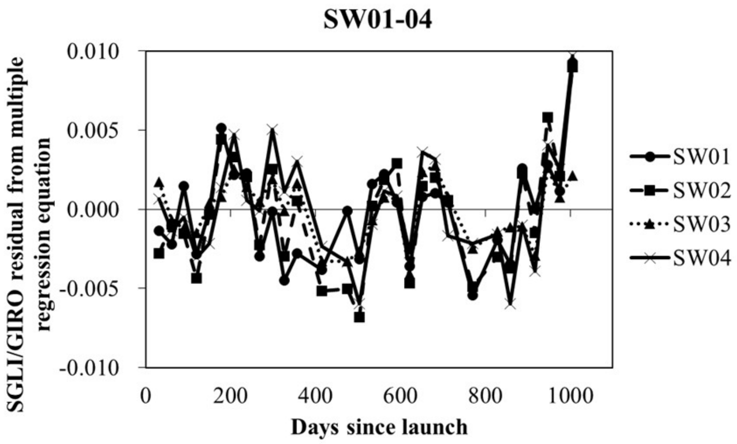

- ✓ The residuals of the regression equation tend to annual variation.
  - This may suggest the effect of libration.

Validation using AHI

- Inter-comparison of SGLI and Himawari8-AHI using GIRO
  - ✓ Inter-comparison of AHI/GIRO and SGLI/GIRO of almost the same observation conditions (obs. time and geometry)
  - ✓ The following differences are corrected by GIRO
    - Geometric conditions (phase angle, libration, sun-moon / moon-satellite distance)
    - Spectral response function of AHI and SGLI

AHI	B01	B02	B03	B04	B05	B06
Wavelength [nm]	470	510	640	860	1600	2300
SGLI	VN04	VN05	VN08	VN11	SW03	SW04
Wavelength [nm]	490	530	673.5	868.5	1630	2210
Ratio SGLI to AHI of lunar irradiance*	1.011	0.983	1.025	1.014	1.037	0.927

  - ✓ Comparison of SGLI/GIRO and AHI/GIRO
    - ➢ 2 cases with almost the same phase angle

Case		date	phase_angle	selenographic latitude of satellite	selenographic longitude of satellite	selenographic latitude of sun	selenographic longitude of sun	dist_sat_moon	dist_sun_moon
①	SGLI	2019/2/20 3:16	8.255	-4.796	1.928	-0.914	-5.368	351544	0.991
	AHI	2019/2/20 3:40	8.262	-3.579	2.260	-0.914	-5.567	398634	0.991
②	SGLI	2019/4/20 0:27	9.342	-6.602	5.118	-1.525	-2.746	364414	1.007
	AHI	2019/4/20 3:00	9.792	-7.067	4.061	-1.524	-4.038	412584	1.007

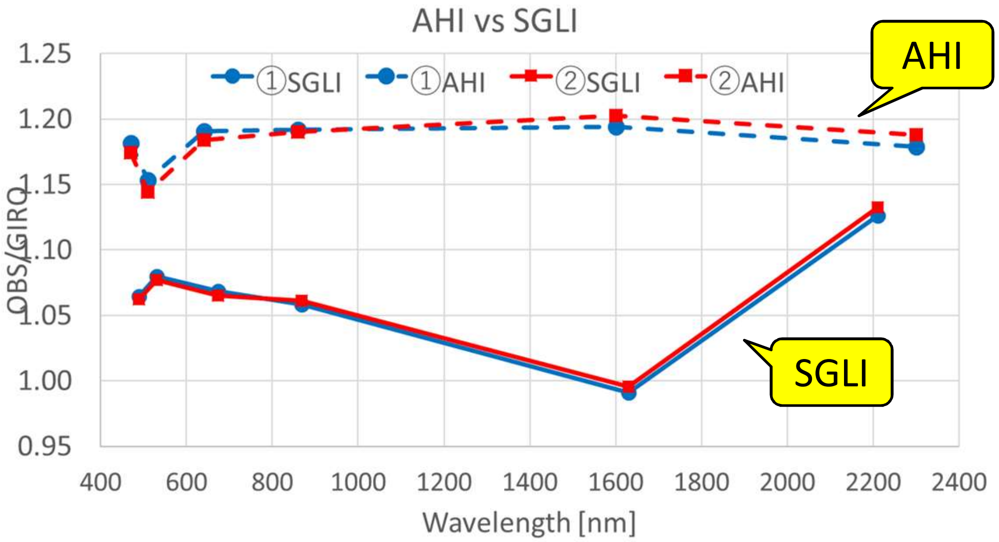

	B01	B02	B03	B04	B05	B06
AHI/SGLI	*11%*	*7%*	*11%*	*12%*	*21%*	*5%*

- AHI results are about 5-20% larger than SGLI.
  - ◆ These results may be include calculation errors of the solid angle and oversampling factor etc.

Validation using AHI

- ☐ Validation of phase angle dependence correction using AHI/GIRO trend

AHI	B01	B02	B03	B04	B05	B06
WL [nm]	470	510	640	860	1600	2300

✓ AHI/GIRO trend (2019)

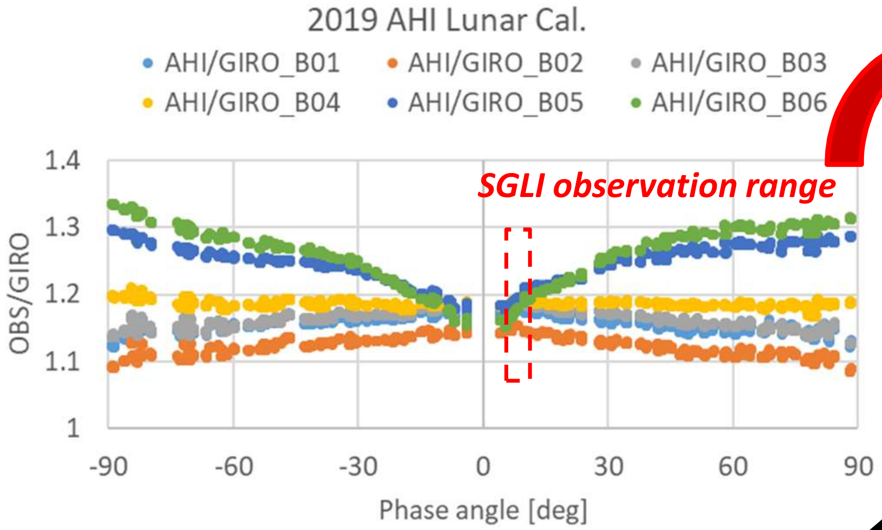

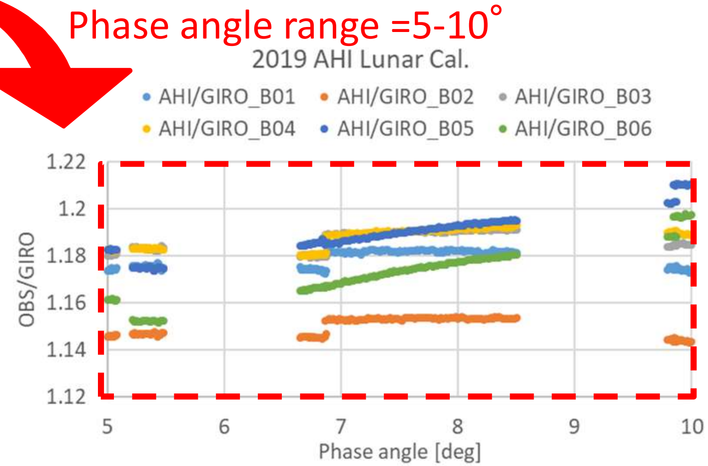

B01

B06

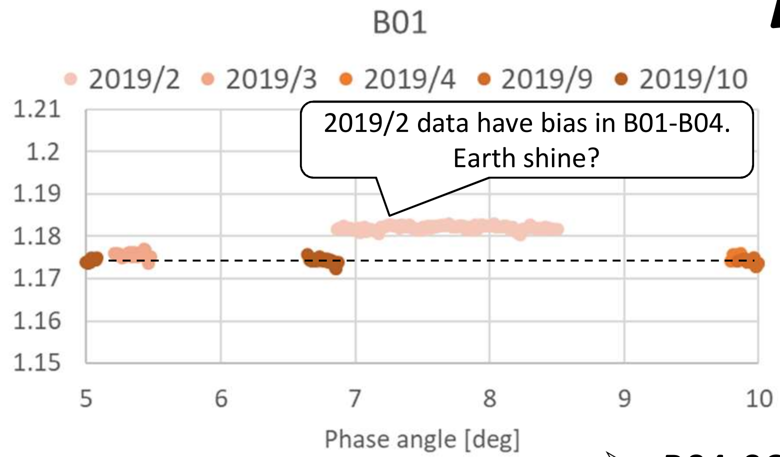

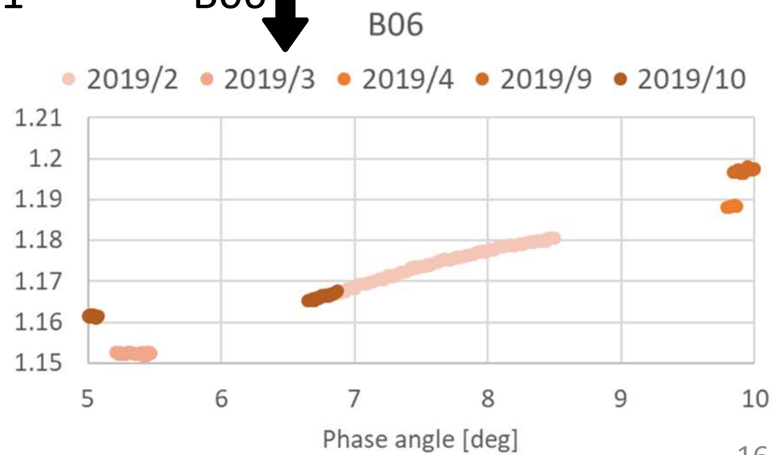

➢ B04-06 trends have phase angle dependence

Validation using AHI

- Validation of phase angle dependence correction using AHI/GIRO trend
  - ✓ Apply himawari-8/AHI data to SGLI simple model

$$f(band, g, day) = \underline{a(band) * g} + \underline{b(band) * day} + \underline{c(band)}$$

➢ AHI/GIRO (Phase angle range =5-10)

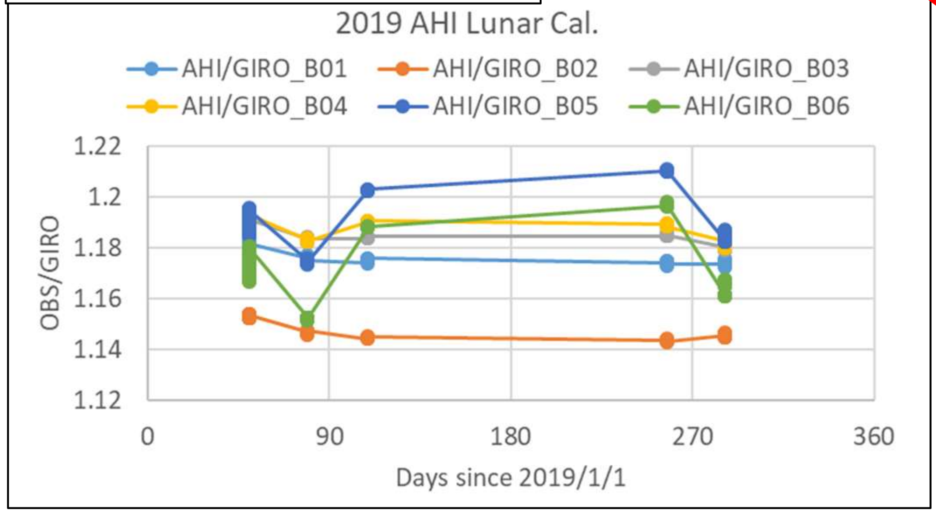

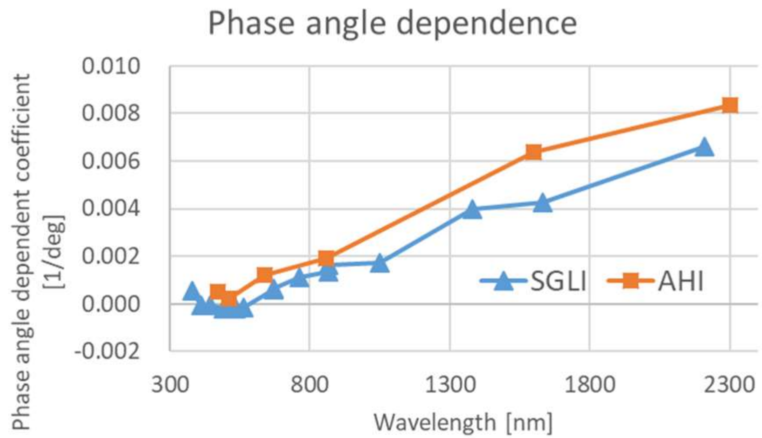

Correction of AHI/SGLI ratio

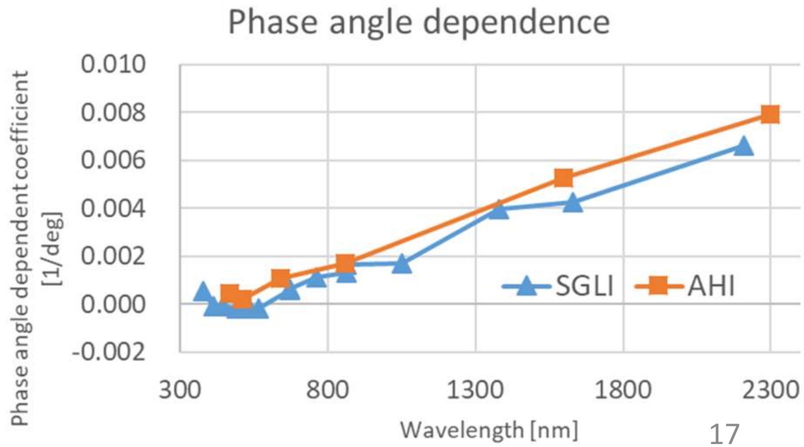

➢ The phase angle dependence coefficient increases with increasing wavelength, and AHI and SGLI have similar tendencies.
  - It suggests that the dependencies are the characteristic of GIRO.
  - In the case of phase angles 5 and 10, without this dependence correction, it becomes the error factors of about 3% {=0.006 x (10-5) @ SW04} in the SWIR.

Conclusion

☐ Conclusion

- ✓ GCOM-C/SGLI continuously observes the moon since the launch , we evaluate the lunar calibration trend using GIRO.
  - These trends show similar trends to other onboard calibrations, suggest that the lunar calibration evaluation acquires the degradation characteristics of the sensor in detail.
  - Similar to the heritage instruments, the OBS / GIRO trend shows phase angle dependence, especially at SWIR band.

- ✓ A simple model was constructed to extract the sensor responsivity degradation from OBS/GIRO trend.
  - As a result, it was confirmed that the phase angle dependence increases as the wavelength increases.
  - These phase angle dependences were verified using AHI/GIRO trend.
  - These results suggest that phase angle dependence corrections are useful for lunar calibration evaluation using GIRO of other sensors observing at the phase angle range of 5-10 degrees.

☐ Future plan

- ✓ These results will be periodically reflected as the radiometric calibration coefficients for the ground processing system.